Available online at www.sciencedirect.com

SciVerse ScienceDirect

Ceramics International 39 (2013) 8153–8158

CERAMICS INTERNATIONAL

www.elsevier.com/locate/ceramint

Influence of Li doping on the humidity response of maghemite (γ-Fe_2O_3) nanopowders synthesized at room temperature

Parag V. Adhyapak*, Vishal Kadam, Umesh Mahadik, Dinesh P. Amalnerkar, Imtiaz S. Mulla*,[1]

Centre for Materials for Electronics Technology (C-MET), Panchawati, off Pashan Road, Pune 411008, India

Received 26 March 2013; accepted 29 March 2013
Available online 9 April 2013

Abstract

Li doped and undoped γ-Fe_2O_3 nanopowders have been synthesized at room temperature via simple method by using ethylene diamine as a precipitating agent. The influence of Li doping on the humidity sensing behavior was investigated by varying the doping concentration of Li (0.15, 0.30, 0.45 and 0.75 mol%). The results revealed that the Li doping was advantageous for tuning the response curves in the lower humidity region. The optimal content for Li doping was found to be 0.45 mol% for which the sensor showed more linear behavior with its potential for device application in comparison with the other samples.

Keywords: γ-Fe_2O_3; Li doping; Ethylene diamine; Humidity sensor

1. Introduction

Humidity sensors have been widely used in many automation systems. A considerable endeavor is being carried out in the development of humidity sensors for application in monitoring relative humidity in moisture-sensitive environments (viz. glove boxes and clean rooms), detection of trace moisture in several kinds of pure gases for semiconductor manufacturing and packaging, cryogenic process, medical and food science application [1–4]. In recent years, the sensor research is mainly focused on the amendment of the performance of humidity sensors with high sensitivity, rapid response, fast recovery and small hysteresis [5–9].

Maghemite (γ-Fe_2O_3) is an n-type semiconductor and has been studied as a sensor material to detect humidity and some combustible and toxic pollutant gases [10–15]. The advantages of the sensor prepared by γ-Fe_2O_3 are high sensitivity, simple design, and low cost. Nevertheless, the major problem associated with this material is its lack of selectivity. To overcome the disadvantage of γ-Fe_2O_3 gas sensor, substantial researches on preparation and doping method of γ-Fe_2O_3 have been done. In general, during humidity sensing, for the activation of the transport mechanisms, the microstructure and the number of water adsorption sites play a fundamental role. These characteristics can be modified by adding suitable dopants to the sensing metal oxide-based material. Neri et al. have extensively investigated the various Fe_2O_3-based humidity sensing materials in presence of dopants with different characteristics such as charges, ionic radii and charge/ionic volume ratios [16–18]. Their investigations suggests that, Li-ions very effectively enhance sensitivity at lower RH due to high polarizing effect of Li^+ ions, resulting into a increased chemisorption of water molecules on the iron oxide surface. Moreover, γ-Fe_2O_3 is also found to be the best suited material for sensing of some gases and organic vapors with some modifiers. For example, Wang et al. [10] reported that the gas sensitivity of γ-Fe_2O_3 to H_2 and LPG was greatly promoted by the addition of Ag_2O and modified with the Al_2O_3 surface-coat doped with PtO via mixture method. Tao et al. [11] studied that gas sensitivity of γ-Fe_2O_3 to alcohol could be increased by doping Y_2O_3 by a sol–gel process. In addition, Niu et al. [12] also found that the rare earth mixed oxides presented good gas sensitivity to gasoline through the sol–gel method in citric acid system. Recently, R.C. Biswal reported the sonochemical precipitation method for preparing pure and Pt doped γ-Fe_2O_3 and found the improved

*Corresponding authors. Tel.: +91 020 25899273; fax: +91 020 25898180.
E-mail addresses: adhyapakp@yahoo.com (P.V. Adhyapak), ismulla2001@gmail.com (I.S. Mulla).
[1]Emeritus Scientist of CSIR, India.

0272-8842/$ - see front matter © 2013 Elsevier Ltd and Techna Group S.r.l. All rights reserved.
http://dx.doi.org/10.1016/j.ceramint.2013.03.089

response of Pt doped γ-Fe_2O_3 towards sub ppm level of acetone at 250 °C [15]. Therefore, one can clearly find that sensitivity of γ-Fe_2O_3 based sensors is strongly dependent on preparation methods and nature of dopant.

In this compass, herein we report the simple room temperature synthesis of Li doped and undoped γ-Fe_2O_3 nanopowders using ethylene diamine as a precipitating agent. The influence of Li doping on the humidity sensing behavior was investigated in detail.

2. Experimental

2.1. Powder synthesis

All the chemicals used in the experiments were of analytical grade. $FeCl_3 \cdot 6H_2O$ (ferric chloride hexahydrate, 99%), $FeCl_2 \cdot 4H_2O$ (ferrous chloride tetra hydrate, 98%), LiCl (lithium chloride 99%), HCl (hydrochloric acid, 37%), ethylene diamine, acetone (99.9%) and de-ionized water were used in the experiments. Typical synthesis procedure is as follows: $FeCl_3 \cdot 6H_2O$ and $FeCl_2 \cdot 4H_2O$ were dissolved in 2 M hydrochloric acid to form an overall concentration of 1 M for $FeCl_3 \cdot 6H_2O$ and 2 M for $FeCl_2 \cdot 4\,H_2O$ in the resultant solution. This ratio of mixed metal ions was kept constant for all the reactions. 0.1 M LiCl solution was prepared separately and added to the Fe^{3+}/Fe^{2+} solution by varying the mol% of Li (0.15, 0.30, 0.45 and 0.75 mol%). Different sets of reactions were performed by drop-wise addition of ethylene diamine (2 M) precursor to this mixed metal ion solution till the pH of the reaction mixture reaches a value >7. All the reactions were accomplished at room temperature. The obtained brown colored products were then filtered, washed with distilled water and acetone and dried at room temperature. The resultant powders were characterized using different physicochemical characterization techniques.

2.2. Powder characterization

The crystalline structures of the resultant powders were characterized by X-ray powder diffraction (XRD) on Rigaku Miniflex Diffractometer using CuK_α radiation ($\lambda = 1.5405$ Å; nickel filter). The crystallite size was estimated using Debye Scherrer Formula. Morphological studies were carried out using Field emission scanning electron microscope (FE-SEM) JEOL-JSM Model 6700F. The particle size distribution analysis was done using a dynamic light scattering method (Ultrafine Particle Analyzer (UPA) from Leeds and Northrup instrument).

2.3. Sensing characterization

Humidity sensing properties of the oxide samples were measured using a closed humidity system. A simple experimental set-up was fabricated which consists of a closed 10 L capacity glass chamber with a neck for inserting a sample under test and a probe of standard Vaisala (Finland) Model HMP 60 humidity meter (humidity range 0–100%RH with an accuracy of 1–5%RH for different humidity ranges). The chamber was kept on an aluminum plate and was made leak-proof by using rubber gasket. The substrates used are 1 cm long and 3 mm diameter ceramic rods having built-in electrodes. The oxide samples were dispersed in ethanol using probe sonicator (Sonic Vibra-Cell) and drop on the ceramic rod. The samples were allowed to dry naturally at room temperature (27 °C) for the evaporation of ethanol. In a typical humidity response measurement the dried sample of undoped and Li doped γ-Fe_2O_3 were inserted in the chamber where humidity was controlled by passing water vapors. After achieving the maximum humidity the water vapor supply was stopped and the phosphorus pentoxide (P_2O_5) was inserted inside the air tight jar for dehumidification. The resistance of the sample with respect to the change in the relative humidity was measured using a digital multimeter. The variations in the resistance with respect to the increase and decrease in the humidity were measured repeatedly.

3. Results and discussions

3.1. Structural and morphological characterization

The structure and Li composition of all Li doped (Li = 0.15, 0.30, 0.45 and 0.75 mol%) and undoped γ-Fe_2O_3 samples synthesized were confirmed with X-ray diffraction (XRD) analyses and the resultant patterns are displayed in Fig. 1. The XRD patterns of all the samples confirm presence of a single-phase γ-Fe_2O_3 with a duly crystalline cubic structure (JCPDS file no. 39-1346). Presence of diffraction peaks at $2\theta = 30.2°$, 35.6°, 43.2°, 53.6°, 57.3° and 62.8° are in good agreement with the corresponding (220), (311), (400), (422), (511) and (440) diffraction planes of γ-Fe_2O_3 and are in accordance with JCPDS data. There is no other phase observed pertaining to Li additive detected within the sensitivity of the instrument, indicating that the Li dissolves into the γ-Fe_2O_3, The broadening of the peaks suggests the nano size nature of the samples and the mean crystallite size calculated using the

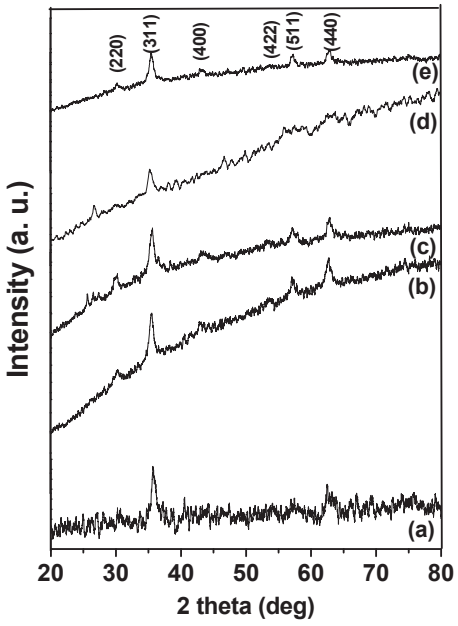

Fig. 1. XRD pattern of (a) undoped γ-Fe_2O_3 and (b) 0.15, (c) 0.30 (d) 0.45 and (e) 0.75 mol% Li doped γ-Fe_2O_3.

Table 1
Lattice parameters of Li doped and undoped γ-Fe_2O_3.

Sr. No.	Sample	Crystallite size (nm)	Lattice parameter, *a* (Å)	Volume (Å^3)
1	γ-Fe_2O_3	36.63	8.347	581.555
2	0.15 mol% Li doped γ-Fe_2O_3	21.10	8.361	581.486
3	0.30 mol% Li doped γ-Fe_2O_3	14.84	8.350	581.182
4	0.45 mol% Li doped γ-Fe_2O_3	18.13	8.350	581.182
5	0.75 mol% Li doped γ-Fe_2O_3	14.44	8.341	581.302

Debye–Scherrer equation

$$D = 0.9\lambda/\beta cos\,\theta$$

where, D is the crystallite size, λ is the wavelength of the incident X-ray beam, β is the true half-peak width in radians and θ is the Bragg's angle. The average crystalline size of the undoped and Li doped γ-Fe_2O_3 is determined to be about 5–10 nm (Table 1).

Table 1 also depicts the lengths of the unit cell parameters of cubic γ-Fe_2O_3 as determined by the X-ray powder diffraction. The cell lengths are in good agreement with the standard data.

Morphology of the Li doped and undoped γ-Fe_2O_3 powders were examined using FE-SEM analyses. Fig. 2 exhibits the FE-SEM images for selective (a) undoped and (b) 0.45 and (c) 0.75 mol% Li doped γ-Fe_2O_3 samples. Predominantly the spherical morphology is observed for all the samples. The diameter of spheres is ~10–15 nm. The clusters of spheres show soft agglomeration. No significant change in the morphology is observed after doping. Particle size distribution from the dynamic light scattering technique (Fig. 3) of representative undoped γ-Fe_2O_3 sample further supports the nano size nature of the sample with particle size range below 100 nm. The results are in accordance with the observed morphological reckoning from the FE-SEM images. The particle size distribution analysis results of the remaining samples (Figures not shown) also confirm the nanostructured nature of the samples.

3.2. Humidity sensing properties

For humidity sensing measurement, all the experiments were carried out at room temperature (27 °C). The change in the resistance was measured for all samples by systematically varying the relative humidity (%RH) in the chamber. The variation in resistance versus %RH (20–90%) plotted for Li doped and undoped γ-Fe_2O_3 is shown in the Fig. 4. For all the samples, the resistance was found to decrease with the increase in the level of relative humidity pertaining to n-type behavior of the samples. The humidity response of undoped sample is shown in Fig. 4(a). Initially, the resistance of the sample decreases slowly from 20% to 50%RH and subsequently (i.e. above 50%RH up to 90%RH) it decreases exponentially upon exposure to humidity, exhibiting an overall change of about 4 orders in magnitude between 20% and 90%RH. The decrease

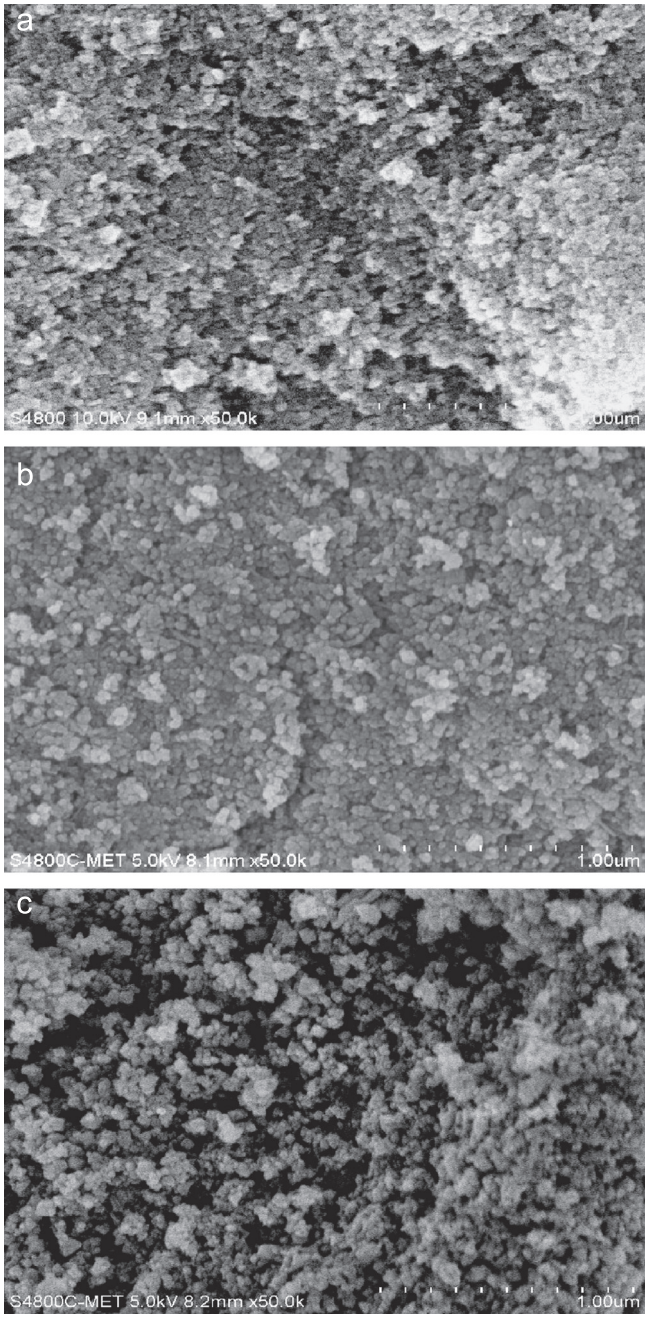

Fig. 2. FE-SEM images of γ-Fe_2O_3 (a) undoped and (b) 0.45 and (c) 0.75 mol % Li doped γ-Fe_2O_3 samples.

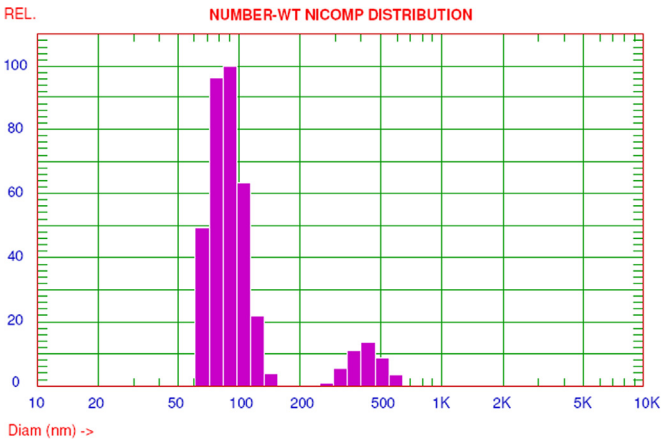

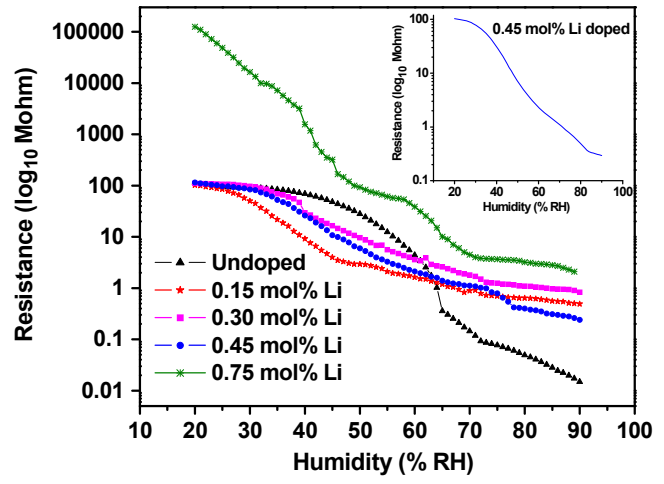

Fig. 4. The variation in resistance versus %RH (20–90%) for Li doped and undoped γ-Fe_2O_3 samples. The inset shows humidity response of 0.45 mol% Li doped γ-Fe_2O_3.

in the resistance on increase in relative humidity from 20% to 90% is 99 MΩ–10 kΩ. Interestingly, the variation in resistance with respect to changes in %RH indicates different shape for the Li-doped samples as compared with the undoped samples. In particular, tuning in the response curves is noted with more linear response in the lower humidity region (20–50%RH). The 0.15, 0.30 and 0.45 mol% Li-doped samples confirm the variation of about 3.5 orders of magnitude between 10% and 90%RH. In general, the resistance values for 0.15, 0.30, and 0.45 mol% Li-doped sample are lower than that of undoped samples. For 0.15 mol% Li doped sample, the total drop in the resistance from 20% to 90% relative humidity is 110 MΩ–100 kΩ, while for 0.30 mol% it is 109 MΩ–800 kΩ and for the 0.45 mol% doped sample it is from 104 MΩ–700 kΩ. Conversely, the total drop in the resistance for 0.15 mol% Li doped sample is found to be 12 GΩ–2 MΩ. Such an abrupt high rise in the resistance in our highest Li doped γ-Fe_2O_3 sample may be attributed to the excess Li probably getting coated on the γ-Fe_2O_3 and/or blocking the pores and ultimately reducing the conduction. These results suggest that the excessive doping was not suitable in making a humidity sensor [19].

We observed the optimal content for Li doping as 0.45 mol % which is in accordance with the reported literature. Moreover, the response curve obtained for 0.45% Li doped sample is more linear (Fig. 4 inset) in comparison with the other samples thus can be considered to have high potential in device application. Hence 0.45 mol% Li doped sample is investigated in more details.

As shown in Fig. 5, the humidity hysteresis characteristics of 0.45 mol% Li doped sample between the humidification and desiccation process was measured in the whole humidity range of 20% to 90% RH. It can be noted that the sensing element exhibits absence of hysteresis loop during cyclic operation from 20% to 60% RH, however, a very narrow hysteresis loop is observed at the humidity range from 65% to 90% RH.

The humidity response and recovery characteristics curve is presented in Fig. 6. The time taken by the sensor to achieve ~90% of the total resistance change is defined as the response time in case of adsorption or the recovery time in case of desorption of the water vapors. The response time (humidification

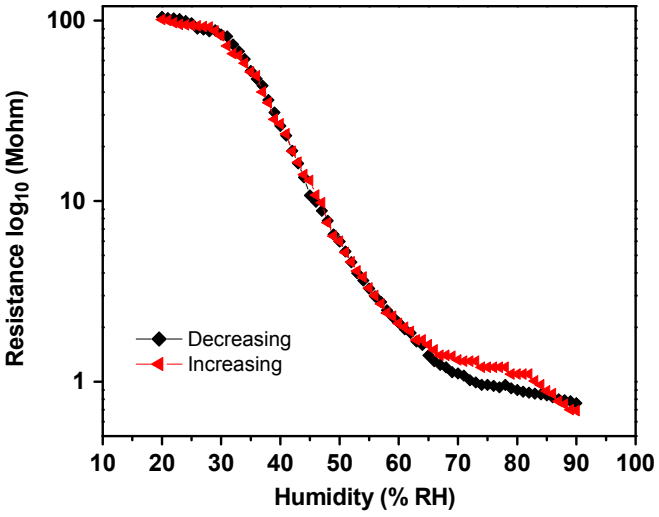

Fig. 5. Humidity hysteresis plots of 0.45 mol% Li doped sample.

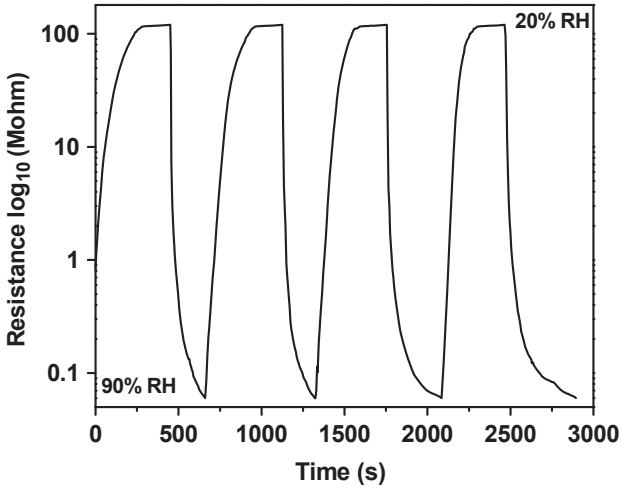

Fig.6. Humidity response and recovery characteristics of 0.45 mol% Li doped sample.

from 20% to 90%RH) was about 150 s, including the equilibrium time of the water vapor inside the test chamber. Therefore, the real response time of the sensor is supposed to be even shorter. Similarly, the recovery time (desiccation from 90% to 20%RH) was about 180 s.

The humidity sensing mechanism for porous ceramic oxides is well reported in the literature [20–22]. The phenomenon of sensing in case of Li doped and undoped samples can be better explained on the basis of surface mechanism. Humidity sensing mechanism is mainly governed by protonic conduction. Water is highly polar as it has lone-pair of electrons and thus, it is a good donor of H^+ and electrons, which is useful in the proton conduction mechanism. Proton is the dominant carrier responsible for the electrical conductivity in the bulk water. On the basis of adsorption and capillary condensation of water, protons are produced. In the ionic sensing materials; as the humidity increases the conductivity increases and the dielectric constant also increases [23,24]. Firstly, water molecules start to physisorb over the hydroxylated surface of oxide by forming a double hydrogen bond. The lowering of resistance can be related to H^+ hopping mechanism. After the formation of monolayer, the successive layer can be adsorbed by a single bond to form an adsorption complex, which subsequently transfers to surface hydroxyl groups. Next water molecule is bonded with two neighboring hydroxyl groups through hydrogen bonding. Thus there is a restriction on the top water molecule layer condensed due to the two-hydrogen bonding. In the second step, water continues to condense on the surface which forms an extra, somewhat un-ordered layer of adsorbed water on the top of the first physically adsorbed water layer. These extra layers vanish the ordering from the initial surface and more and more protons become free to move inside the condensed water. Here the addition of Li plays an important role. Li ion strongly favors the increase of the number of chemisorption sites for the water vapors due to its small size and the high local charges [25]. Moreover, addition of Li ions also contributes in increasing the protonic conduction and reorientation of the water molecules. It is well known that in the case of Li doped samples the mechanism is ionic-type [26].

To check the reproducibility of the sensor, five samples were made and tested for the humidity sensing characteristics. All the samples show similar response. The samples did not show any change in the current on exposure to other gases like H_2, liquefied petroleum gas (LPG), and ethanol at room temperature, thus exhibiting high humidity response without any interference from gas is an added advantage for the commercial application of this material. Furthermore, it is also seen that over major part of humidity (relative humidity between 30% and 80%) the overall response toward humidity is very systematic. This type of variation with respect to humidity is useful for its usage in electronic devices.

4. Conclusions

It is demonstrated that a facile room temperature synthesized γ-Fe_2O_3 nanostructured material on doping with Li gives improved response towards humidity. Room temperature synthesis with the help of ethylene diamine as a precipitating agent was proven to be advantageous in comparison with other high temperature synthesis methods since it helps in retaining the porosity. The amount and distribution of Li species seems to be one of the decisive factors in responding humidity. The results strongly suggest that humidity sensitivity can be tuned by mere doping of lithium ions. We assume that the porosity attended at the time of low temperature synthesis is retained unlike the one wherein the samples are processed at the higher temperatures.

Acknowledgments

Imtiaz S. Mulla, gratefully acknowledges CSIR, New Delhi, India for awarding him *Emeritus Scientist* Scheme.

References

[1] Y.C. Yhe, T.Y. Tseng, Analysis of the d.c. and a.c. properties of K_2O-doped porous $Ba_{0.5}Sr_{0.5}TiO_3$ ceramic humidity sensor, Journal of Materials Science 24 (1989) 2739–2745.
[2] Y. Sadako, M. Matsuguchi, Y. Sakai, H. Aono, S. Nakayama, H. Kuroshima, Humidity sensor using KH_2PO_4-doped porous (Pb, La)(Zr, Ti)O_3, Journal of Materials Science 22 (1987) 3685–3692.
[3] S. Upadhyay, P. Kavitha, Lanthanum doped barium stannate for humidity sensor, Materials Letters 61 (2007) 1912–1915.
[4] P.G. Su, S.C. Huang, Humidity sensing and electrical properties of a composite material of SiO_2 and poly-[3-(methacrylamino) propyl] trimethyl ammonium chloride, Sensors and Actuators B 105 (2005) 170–175.
[5] H.W. Chen, R.J. Wu, K.H. Chan, Y.L. Sun, P.G. Su, The application of CNT/ Nafion composite material to low humidity sensing measurement, Sensors and Actuators B 104 (2005) 80–84.
[6] Y. Li, M.J. Yang, A novel highly reversible humidity sensor based on poly (2 propyn-2-furoate), Sensors and Actuators B 86 (2002) 155–159.
[7] M.J. Yang, Y. Li, N. Camaioni, G.G. Miceli, A. Martelli, G. Ridolfi, Polymer electrolytes as humidity sensors: progress in improving an impedance device, Sensors and Actuators B 86 (2002) 229–234.
[8] J.M. Corres, F.J. Arregui, I.R. Matias, Sensitivity optimization of tapered optical fiber humidity sensors by means of tuning the thickness of nanostructure sensitive coatings, Sensors and Actuators B 122 (2002) 442–449.
[9] X. Wang, J. Zhang, Z. Zhu, J. Zhu, Humidity sensing properties of Pd^{2+} doped ZnO nanotetrapods, Sensors and Actuators B 253 (2007) 3168–3173.
[10] J.Z. Wang, M.S. Tong, X.Q. Wang, et al., Sensors and Actuators B 84 (2002) 95.
[11] S.W. Tao, X.Q. Liu, X.F. Chu, Y.S. Shen, Sensors and Actuators B 61 (1999) 33.
[12] X.S. Niu, W.M. Du, W.P. Du, Sensors and Actuators B 99 (2004) 399.
[13] T.S. Zhang, H.M. Luo, H.X. Zeng, et al., Sensors and Actuators B 32 (1996) 181.
[14] Y. Nakatani, M. Matsuoka, Japanese Journal of Applied Physics 22 (1983) 233.
[15] R.C. Biswal, Pure and Pt-loaded gamma iron oxide as sensor for detection of sub ppm level of acetone, Sensors and Actuators B 157 (2011) 183–188.
[16] G. Neri, A. Bonavita, S. Galvagno, C. Pace, S. Patan'e, A. Arena, Humidity sensing properties of Li–iron oxide based-thin films, Sensors and Actuators B 73 (2001) 89–94.
[17] G. Neri, A. Bonavita, C. Pace, S. Patan´e, A. Arena, M. Allegrini, S. Galvagno, Iron oxide based-thin films for humidity sensors, in: Proceedings of the XIII Eurosensors Conference, 1999, pp. 149–152.

[18] G. Neri, A. Bonavita, S. Galvagno, N. Donato, A. Caddemi, Electrical characterization of Fe_2O_3 humidity sensors doped with Li^{2+}, Zn^{2+} and Au^{3+} ions, Sensors and Actuators B 111–112 (2005) 71–77.
[19] L. Wang, D. Li, R. Wang, Y. He, Q. Qi, Y. Wang, T. Zhang, Sensors and Actuators B 133 (2008) 622–627.
[20] B. Kulwicki, Humidity sensors, Journal of the American Ceramic Society 74 (1991) 697–708.
[21] E. Traversa, Ceramic sensors for humidity detection: the state-of-the art and future developments, Sensors and Actuators B 23 (1995) 135–156.
[22] T.H. ubert, Humidity-sensing materials, MRS Bulletin 24 (1999) 49–54.
[23] F. Ansbacher, A.C. Jason, Nature 24 (1953) 177.
[24] J.M. Thorp, Transactions of the Faraday Society 55 (1959) 442.
[25] W.J. Fleming, A Physical Understanding of Solid-State Humidity Sensors, SAE Paper no. 810432, 1981, pp. 51–62.
[26] Y. Yamamoto, K. Murakami, Humidity sensor using TiO_2–SnO_2 ceramics, in: T Seiyama (Ed.), Chemical Sensor Technology, Elsevier, Tokyo, 1989.